



Molecular Dynamics Investigation of Bonded Twist Boundaries*

KURT SCHEERSCHMIDT AND VOLKER KUHLMANN

Max Planck Institute of Microstructure Physics, Weinberg 2, D-06120 Halle, Germany

schee@mpi-halle.de

vkuhl@mpi-halle.de

Abstract. Molecular dynamics simulations using empirical potentials have been performed to describe atomic interactions at interfaces created by macroscopic wafer bonding. Misalignment due to relative twist rotation of the wafers influences the bondability of larger areas. Depending on the twist angle the bond energy varies and different defect and atomic arrangements at the interfaces occur. In addition, if very thin wafers are being bonded the free surfaces are modified by the resulting interface relaxation.

Keywords: wafer bonding, molecular dynamics, twist, screw dislocation, dreidl

1. Introduction

Wafer bonding, i.e. the creation of interfaces by joining two wafer surfaces, has become an attractive method for many practical applications in microelectronics, micromechanics or optoelectronics. The macroscopic properties of bonded materials are mainly determined by the atomic processes at the interfaces during the transition from adhesion to chemical bonding. Thus, the description of the atomic processes is of increasing interest to support the experimental investigations or to predict the bonding behavior.

It is possible to use quantum-theoretical *ab initio* calculations with a minimum of free parameters to predict material properties of small systems. The only practical method to simulate atomic processes with macroscopic relevance, however, is classical molecular dynamics (MD) using suitably fitted empirical many-body potentials. Basically, MD integrates the Newtonian equation of motion with a fifth-order predictor-corrector algorithm using time steps in the order of *fs*. The procedure used here is outlined e.g. in [1] together with further references of successfully applying MD-simulations to wafer bonding. Such simulations make a sufficiently large number of particles and relaxation times up to μs

accessible, even though the electronic structure and the nature of the covalent bonds can only be described indirectly. However, it is important to find physically motivated semi-empirical potentials, using the moments of the electron density in tight-binding representations [2–4], or fitted with data of the density functional theory in the local density approximation (DFT-LDA). Based on the MD relaxed model, conventional transmission (TEM) and high resolution (HREM) electron microscope structure imaging has been applied to investigate the resulting interfaces and defects at an atomic level [5].

Whereas bonding of two perfectly aligned, identical wafers give a single, perfectly bonded wafer without defects [6], miscut of the wafer results in steps on the wafer surfaces and thus edge dislocations at the bonded interfaces are created. Bonding wafers with rotational twist leads additionally to a network of screw dislocations at the interface. The present paper investigates the interface bonding of silicon wafers as a function of the twist angle and the thickness of the wafers in more detail.

2. The Bonded Interface with 90° Twist Rotation

Misalignment of the wafers during wafer bonding leads to bonded interfaces with twist rotation. A special

*Presented at the “Euro Conference on Structure and Composition of Interfaces in Solids,” Schwäbisches Bildungszentrum Kloster Irsee, Germany, 19.-23.8.2002

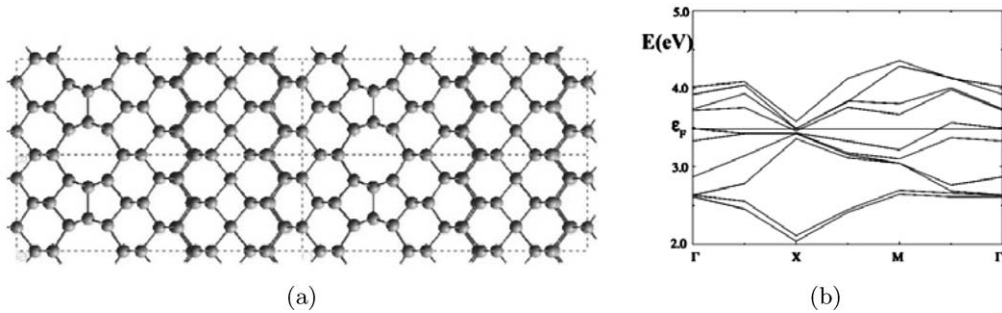


Figure 1. MD simulated structural model (a) of the $Pmm(m)$ interface at 90° twist and corresponding DFT band structure (b).

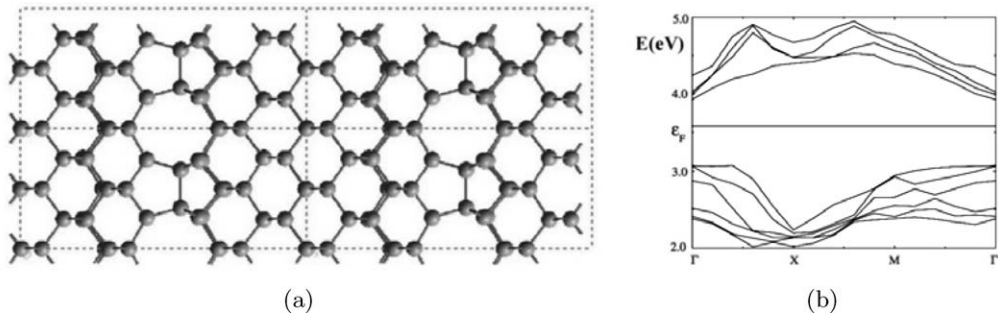


Figure 2. MD simulated structural model (a) of the $P(\bar{4})m2$ interface at 90° twist and corresponding DFT band structure (b); The dreidl structure reduces the interface energy by approximately 20%.

situation is the 90° twist, which inherently occurs between monoatomic steps. As presented earlier [1], the Stillinger-Weber potential [7] applied to a 90° twist bonded wafer pair yields a metastable fivefold coordinated interface with a mirror symmetry normal to the interface characterized by a $Pmm(m)$ layer group (Fig. 1). Using the Tersoff [8, 9] or bond-order like [2] potentials and metastable or well-prepared starting configurations allows further structure relaxation and energy minimization. Figure 2 shows this relaxed configuration, which is (2×2) reconstructed and consists of structural units with a $\bar{4}2m$ -($D2d$) point group symmetry, called the $\bar{4}2m$ -dreidl. The dreidl fits two rotated half crystals of minimal structural disorder and fourfold coordination described by a $P(\bar{4})m2$ layer symmetry. The interface energy is reduced by approximately 20%. The detailed structural and energetical characterization of the different structural units found by empirical MD are discussed in [10]. It should be emphasized that the dreidl structure is found to be the minimum energy configuration also in *ab initio* DFT-LDA simulations [1]. However, the energies differ from those given in [10]: one yields 0.45 J/m^2 and 1.39 J/m^2 for the $P(\bar{4})m2$ and

the $Pmm(m)$ configurations, which is 50% less or 20% higher than the corresponding values using Tersoff potentials. Much more important is the modification of the band structure due to the different interface relaxation which may enable tailoring of the electronic properties: whereas the metastable configuration of Fig. 1 yields semi-metallic behavior, the dreidl structure of Fig. 2 yields a larger band gap than in perfect lattices.

3. Wafer Bonding with Small Twist Rotational Misalignment

The effect of a small twist angle as a rotational misorientation results in a checkerboard-like interface structure [11]. The simulation of wafer bonding starts with two Si blocks that are separated by a few Å and may have dimerized (100)-surfaces. Figures 3 and 4 show some of the resulting minimum structures gained for higher annealing temperatures¹ and different twist rotation angles. Before the bonding process takes place, the superposition of the two wafers looks like a Moiré pattern in the projection normal to the interface. After bonding and sufficient relaxation under slow heat

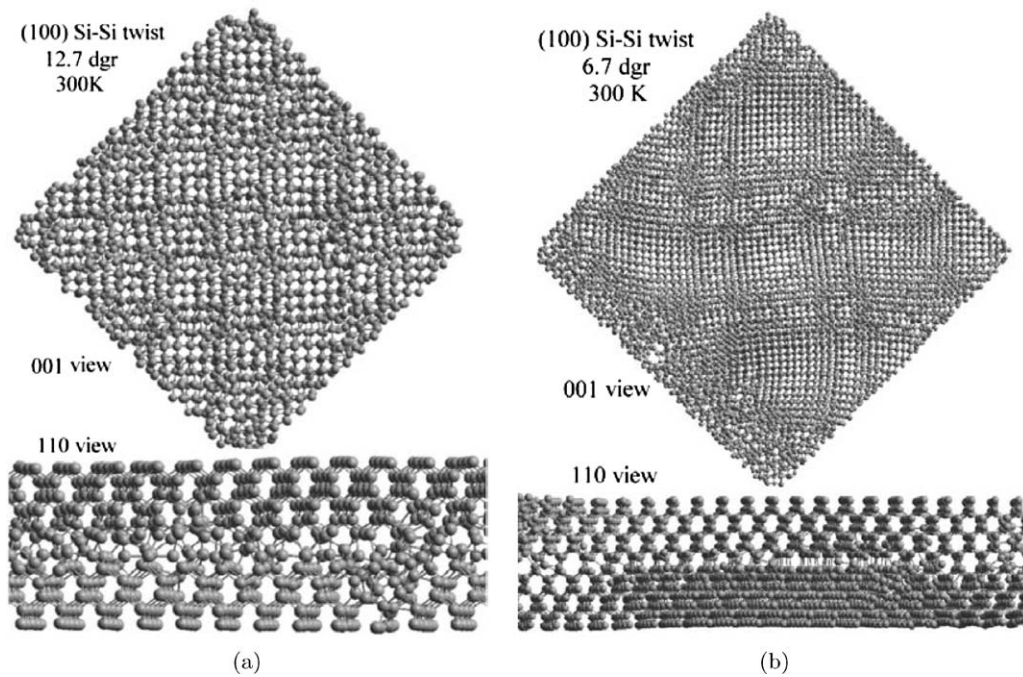


Figure 3. MD simulated structural models ([001] and [110] views) of bonded wafers with different rotationally twist angles annealed at 300 K for parallel dimer start configurations: (a) 12.7° , 6500 atoms, 4.9 nm box; (b) 6.7° , 23000 atoms, 9.2 nm box.

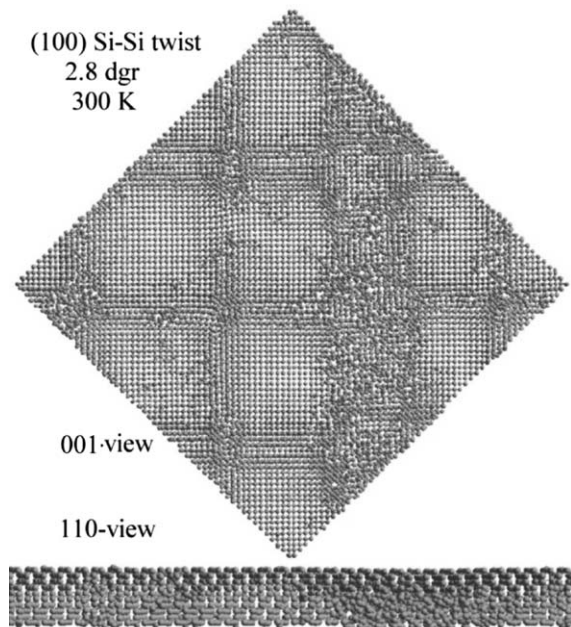


Figure 4. MD simulated structural model ([001] and [110] view) of bonded wafers with a 2.8° rotationally twist angle annealed at 300 K for parallel dimer start configurations: 134500 atoms, 22 nm box with additional bonding over steps along [110] indicated by the broad band at the right.

transfer conditions, almost all atoms have a bulk-like environment separated by screw dislocations, which may have a high rate of kinks. The screw dislocation network has a period half of the initial Moiré accommodating the twist. One reveals the more localized imperfectly bonded regions around the screw dislocations for smaller twist angles, whereas bonding at higher angles result in more or less widely spread strained interface regions. In contrast to the case of very thin bonded wafers, where the relaxation of the screws seems to be perfect (cf. Chap. 4), the widely spread defect regions with the high kink rate looks like metastable more complex configurations and can only be revealed having the dislocation properties indirectly by the simulated electron microscope image contrasts as discussed lateron.

Whereas all simulations shown in Figs. 3–5 with parallel dimerization at start clearly demonstrate the creation of the screw dislocation network, for orthogonal dimerization or small twist angles this is no longer valid. In Fig. 5 bonding with orthogonal start configurations (a and b) are compared with parallel dimer start configurations (c and d). Thus the bonding of Figs. 5(a) and (b) may be considered as bonding with an additional 90° twist rotation. Clearly the periodicity of the defect region is twice of those of (b and c) smoothing out the interface, but creating additional shear strains.

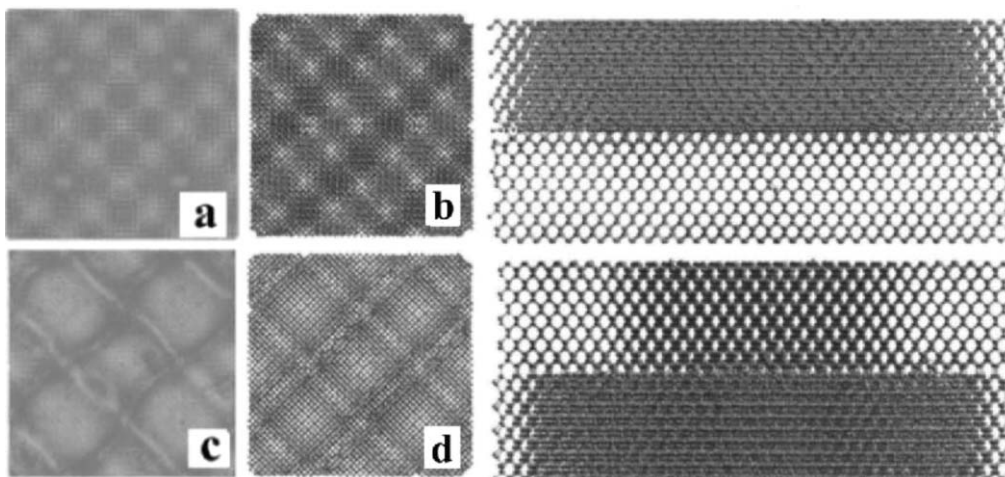


Figure 5. MD relaxations of bonding rotationally twisted wafers ([001] views and in addition for (b) and (d) [110] views, resp.) with different angles: (a) 2.8°, 134500 atoms, 22 nm box, orthogonal dimers, (b) 6.7°, 9.2 nm box, orthogonal dimers in start, i.e. an additional 90° twist; (c) as (a) and (d) as (b) with parallel dimer start configuration.

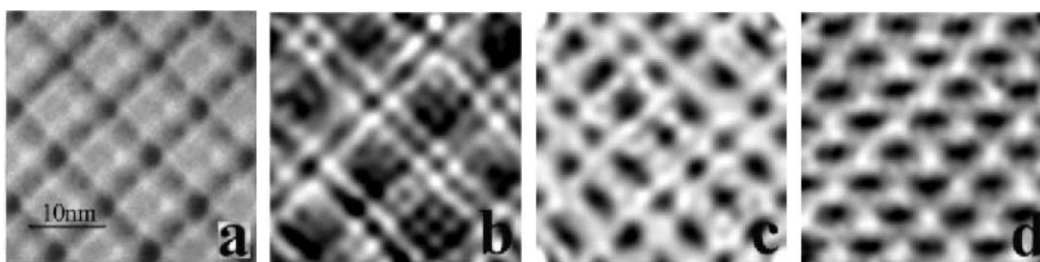


Figure 6. Experimental 400kV bright-field diffraction contrast (a) of a 2.4°-twist bonded interface (Courtesy: R. Scholz, MPI-Halle) and simulated TEM images (b-d, 400kV, thickness $t \sim 40$ nm, varying beam tilt) of models as b and d from Fig. 5: (b) parallel dimers in start configurations, 4.6°-twist, 13.5 nm box, (c,d) orthogonal dimers in start configuration, 6.7°-twist, beam along zone axis and tilt into [200]-excitation, respectively.

Independently from the chosen twist angles and box dimensions all final structures yield bond energies of approximately 4.5 eV/atom at 0 K, however, varying slightly with the twist angle. A maximum occurs between 4° and 6° twist related to a change of the bonding behavior itself. The higher the annealing temperature the better the screw formation. Figure 6 shows an experimental bright-field electron diffraction contrast image of an interface bonded under UHV-conditions compared with simulated plan view TEM contrasts based on the relaxed structure, assuming different beam orientations [hkl] relative to the zone axis [001]. By using simulated plan view TEM based on the relaxed interface models Fig. 6 demonstrates the dislocation like contrast of even the extended defect regions and that a detailed structure investigation is enabled by applying suitable imaging conditions (cf. e.g. [12]).

4. Twist Wafer Bonding of Very Thin Layers

In contrast to the simulations of the bonding process of two bulk wafers presented in the preceding chapter, the MD simulation of bonding thin wafers yields effects at the free surfaces, not compensated by the avalanche effect as for much thicker crystal lattices. Two wafers of 8 atomic layers thickness are taken, one of them having the lowest layer fixed to approximate the continuation into a large bulk. The Figs. 7 and 8 demonstrate the wafer bonding of a very thin slice on top of a bulk support. Depending on the chosen rotational twist of 2.8°, 6.7° and 12.7°, the plan views of the initial configurations (cf. Fig. 7(a)) and the MD relaxed models (cf. Fig. 9(a), (b) and 7(b)) reveal Moiré patterns and screw dislocation networks with varying periodicity, respectively. The separation of the screw

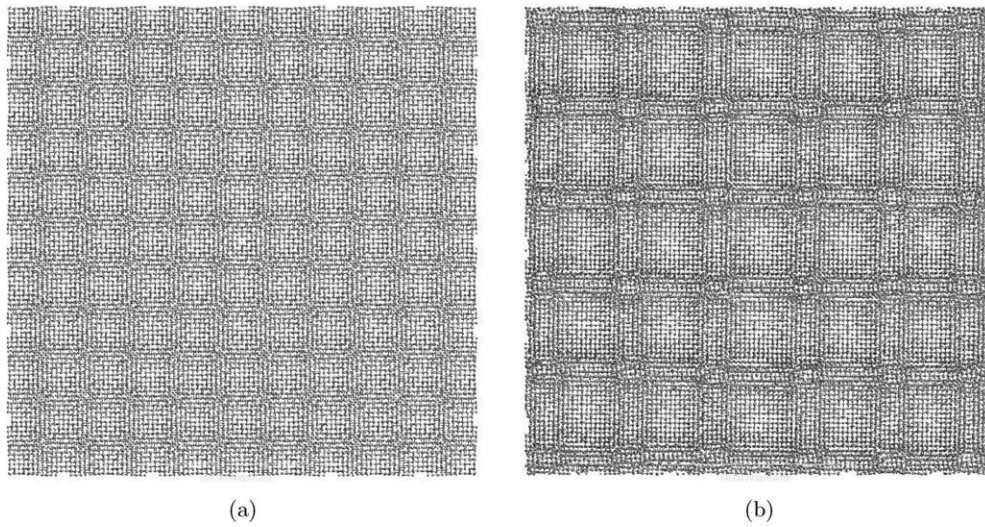


Figure 7. Simulation of thin bonded wafers with 6.7° rotational twist: [001] view of initial (a) and MD-relaxed (b) model showing the resulting screw network.

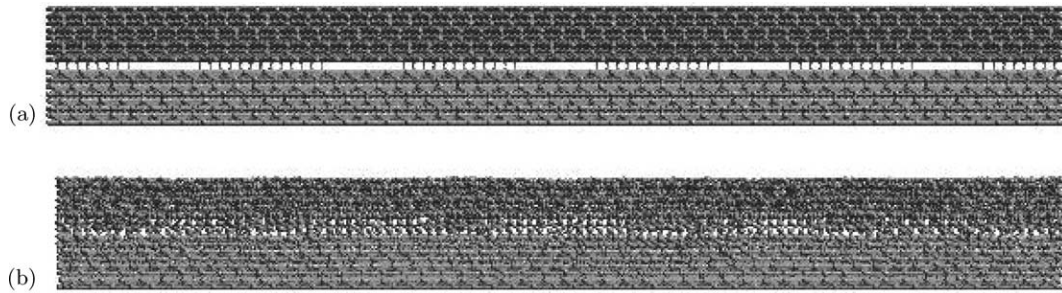


Figure 8. Simulation of thin bonded wafers with 6.7° rotational twist: [110] projections of initial (a) and MD-relaxed (b) model showing bonding details at the interface.

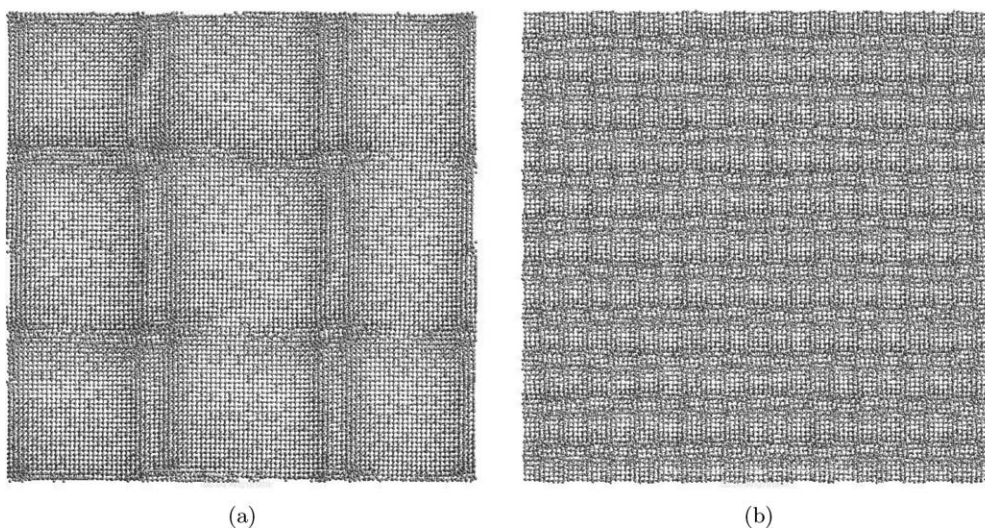


Figure 9. MD-simulation of bonding thin wafers with rotational twist: [001] view of MD relaxed model with 2.8° (a) and 12.7° (b) twist.

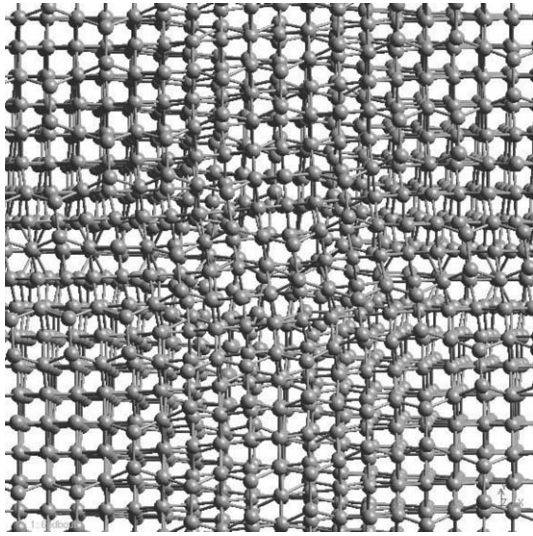


Figure 10. A typical node of $[110]$ - and $[\bar{1}10]$ -screw dislocation intersection of the 6.7° twist bonded interface resulting from MD simulated bonding of thin wafers.

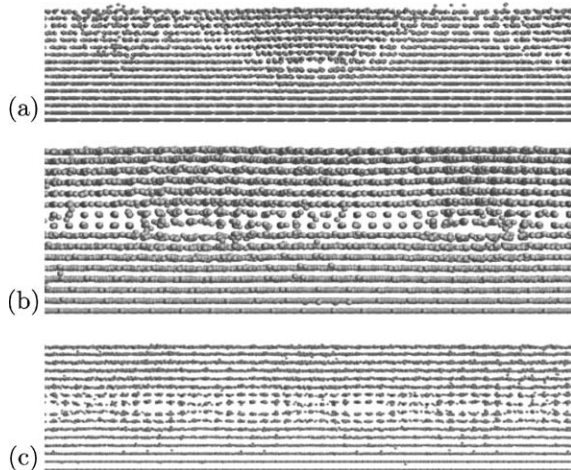


Figure 11. Interfaces after MD-relaxation of thin bonded wafers with 2.8° , 6.7° and 12.7° twist (a,b,c) in $[110]$ projection showing the different defect core structures.

dislocations for all three angles relates to the periodicity of the corresponding Moiré pattern of the initial (un-bonded) models, being twice as large (cf. Fig. (7(a) and (b))). The visual Moiré pattern originates from the wafer periodicity projected onto the $[001]$ plane, while the screw dislocation network derives from the structural periodicity at the interface (period of a projected zinc blende structure is half as big as period of zinc blende itself). The cross section in $[110]$ projection of

the 6.7° twist bonded interface along the dislocation lines (cf. Fig. 8(a) and (b)) illustrate both the perfect bonding in areas between the dislocations, and the periodicity. In addition, a corrugation of the free surfaces of the thin layer may be revealed, a feature not observed on thick wafers. The cross-sectional views in Fig. 11(a)–(c) demonstrate the corrugation effects in detail for three selected regions. Along the screw dislocations (perpendicular to the image plane) the bonding distance between the wafer increases slightly, indicating varying strains within the wafer. This results in an additional displacement of the atomic planes close to the screw dislocation, which for thin wafers extends towards the surface. It diminishes with increasing distance from the interface and will thus vanish for increasing thickness of the bonded wafers. Both, the large scale dislocation network (cf. Fig. 7(b)) and the geometry of the dislocation intersections (nodes) (cf. Fig. 10) show similarities to results from earlier analysis [13] of perfect screw dislocation networks inserted into perfect crystals. That means the dislocation network in thin layer bonding is better relaxed towards perfect screw dislocations than it was obtained for thick wafers.

5. Conclusions

Molecular dynamics simulations (MD) based on empirical potentials are used to investigate the bonding of two Si(001) wafers rotationally misaligned. Calculated bonding energies and forces strongly depend on the starting twist and result in special interface configurations no longer perfectly coordinated. The simulations lead to a better understanding of the physical processes at the interfaces and support the experimental investigations, especially the electron microscope structure analysis. In addition, thin wafers have been simulated. Unlike bonding bulk wafers, the MD simulations for thin wafers yield effects at the free surfaces, like corrugation and straining, not compensated by the avalanche effect.

Note

1. Erratum: Due to a scaling error the maximum annealing temperatures in the earlier paper [11] are given with wrong numbers, instead 2100 K only room temperature was used, the correct simulations with higher annealing temperatures will be repeated in a forthcoming paper.

References

1. K. Scheersmidt, D. Conrad, and A. Belov, *Comp. Mat. Science* **24**, 33 (2002).
2. D. Conrad and K. Scheersmidt, *Phys. Rev. B* **58**, 4538 (1998).
3. D.G. Pettifor and I.I. I.I. Oleinik, *Phys. Rev. B* **59**, 8487 (1999).
4. D. Conrad, K. Scheersmidt, and U. Gösele, *Appl. Phys. Lett.* **77**, 49 (2000).
5. K. Scheersmidt, D. Conrad, A. Belov, and H. Stenzel, in *Electrochem. Soc. Proc.*, (1998), vol. 97, no. 36, p. 381.
6. D. Conrad, K. Scheersmidt, and U. Gösele, *Appl. Phys. A* **62**, 7 (1996).
7. F.H. Stillinger and T.A. Weber, *Phys. Rev. Lett.* **31**, 5262 (1985).
8. J. Tersoff, *Phys. Rev. B* **38**, 9902 (1989).
9. J. Tersoff, *Phys. Rev. B* **39**, 5566 (1989).
10. A.Y. Belov, D. Conrad, K. Scheersmidt, and U. Gösele, *Philos. Magazine A* **77**, 55 (1998).
11. K. Scheersmidt, in *Mat. Res. Soc. Symp. Proc.* vol. 681E, in print, 2001.
12. K. Rouviere, J.L. Rousseau, F. Fournel, and H. Moriceau, *Appl. Phys. Lett.* **77**, 1135 (2000).
13. A.Y. Belov, K. Scheersmidt, and U. Gösele, *Phys. Status Solidi (a)* **171**, 159 (1999).